



## QUANTIFYING BIOFILM STRUCTURE

Zbigniew Lewandowski, Derek Webb, Martin Hamilton  
and Gary Harkin

*Center for Biofilm Engineering, Montana State University, Bozeman,  
MT 59717-3980, USA*

### ABSTRACT

This article defines some quantitative parameters for describing the structure of a biofilm. The parameters can be calculated from a two-dimensional cross-sectional image on a plane parallel to the substratum within an *in situ* biofilm. Such images can be acquired using a confocal scanning laser microscope (CSLM). The parameters will eventually be used for eliciting relationships between the biofilm's structure and its biochemical function, and for computer model evaluation. The results shown here indicate that the structural parameters appear to be reaching steady-state conditions as the biofilm grows to a steady state. © 1999 IAWQ Published by Elsevier Science Ltd. All rights reserved

### KEYWORDS

Biofilm; structure; quantitative morphology; shape; image analysis.

### INTRODUCTION

Advances in microscopy, particularly the advent of the Confocal Scanning Laser Microscope (CSLM), and sophisticated computer image analysis tools have permitted visualization of biofilm structure to an extent that was impossible a decade ago (Lawrence *et al.*, 1991). Recent CSLM investigations of biofilm have shown that many biofilms possess a heterogeneous structure (Costerton, *et al.*, 1994). For example, at the substratum, the biofilm cells can be arranged in a thin, dense layer of cells, to which are bound some dense, roundly shaped, microcolonies, filled with extracellular polymers, packed with microorganisms, and separated by interstitial voids. The space within the voids is filled with water or with low concentrated extracellular polymers. The interstitial voids are interconnected, forming a network of channels that create a characteristic porous structure. This description is consistent with the observations of various research groups (Keevil and Walker, 1992; Wolfaardt *et al.*, 1994; Massol-Deya, 1994).

The reasons for structural heterogeneity are largely unknown, but they undoubtedly involve both physical and biological factors. Van Loosdrecht *et al.* (1995) discusses how the substrate loading rate, shear stress, and growth rate may influence the biofilm structure. It may be that biological mechanisms create a structure that maximizes mass transport to deep layers within the biofilm. It has been well documented that the structural heterogeneity influences the mass transport mechanism and rates near and within biofilms (Bishop and Rittmann, 1995; Lewandowski *et al.*, 1994; Zhang and Bishop, 1994a; Yang and Lewandowski, 1995; deBeer *et al.*, 1994). The evidence is just emerging to suggest that biofilm heterogeneity indeed reflects a biological mechanism (Davies *et al.*, 1998).

Quantifying the structure of biofilms is an important step towards understanding and describing biofilm systems. Zhang and Bishop (1994 a,b) determined the densities, porosities, specific surface area, and mean

pore radius of biofilms. Hermanowicz *et al.* (1995) used CSLM images to estimate the fractal dimension from microscope images and biofilm morphology. Piciooreanu *et al.* (1998) defined both two- and three-dimensional parameters, such as surface enlargement, surface roughness, fractal dimension, porosity, and compactness, for purposes of describing the structure of computer simulated biofilms.

The structural elements of the biofilm that one might choose to measure are called features. Biomass cluster size and cluster shape are examples of features. Structural features are naturally visual, and they possess characteristics such as size, shape, color and texture that may possibly be expressed quantitatively. The calculation of meaningful quantities may be complicated and require the power of a modern computer. There are many structural features that one could choose to study, and an objective strategy is required to select the most useful ones. One way to evaluate the relevance of a feature is by how well it correlates with changes in the underlying processes that created the biofilm. An alternative is to choose features that may be correlated with biofilm function, where function is measured, for example, by using microelectrode probes to ascertain local concentrations of relevant chemicals. Features should be related in some manner to the underlying processes in order to be of scientific significance. There are some obvious starting points. It is reasonable, for example, to believe that the size of biomass clusters or interstitial spaces might be associated with variations in species or nutrition, and that the shape of clusters might be associated with hydrodynamics. It is important to avoid visually interesting features that cannot be related to underlying biological, chemical or physical processes; time spent creating measures of those features will probably not lead to scientific insights.

We conjecture that there exist a finite number of features, and associated quantitative measures, that describe the structure of a biofilm and contain enough information either to reflect variations in the growth dynamics or to predict the functional characteristics of the biofilm. As a starting point in finding such features, we rely on the fact that biofilms achieve steady-state conditions, where the physical structure is dynamic at the molecular level, but static as the scale corresponding to our microscopic field of view. If a parameter (measured feature) appears to approach steady state, it is behaving in the expected manner, and it has passed our initial screening test. If it does not, we provisionally reject the parameter, assuming it is not a useful descriptor of biofilm structure.

This paper describes our experience in defining, calculating, and using quantitative biofilm structure parameters based on two-dimensional, cross-section images of a biofilm captured using a light microscope. The goals are to: (1) define the parameters, (2) describe computer software that we created to calculate the selected parameters from microscope images of fully hydrated, heterogeneous biofilms, and (3) observe whether the parameters reflect the structural changes evident when a biofilm grows to steady state.

## METHODS

### Biofilm growth

An open channel reactor, made of polycarbonate, 4.5 cm deep, 5 cm wide, and 55 cm long was used. The nutrient solution was made of  $\text{KH}_2\text{PO}_4$  (0.69 mM),  $\text{K}_2\text{HPO}_4$  (1.5 mM),  $(\text{NH}_4)\text{SO}_4$  (0.079 mM),  $\text{MgSO}_4 \cdot 7\text{H}_2\text{O}$  (0.013 mM), glucose (0.040 g/L), and yeast extract (0.031 g/L). The inoculum, 1 mL of frozen stock culture (from the Center for Biofilm Engineering) consisted of: *Pseudomonas aeruginosa*, *Pseudomonas fluorescens*, and *Klebsiella pneumoniae*. The reactor was operated batchwise for 12 h and then switched to the continuous flow mode. Biofilms were grown at a flow velocity 2 cm/sec for 18 days. Flow velocity was maintained by recycling the growth medium using peristaltic pumps (Cole-Parmer, Chicago, IL). The nutrient solution was aerated in the mixing chamber. A glass slide was placed in the bottom of the middle of the reactor where measurements were taken.

### Microscopic analysis

The reactor was permanently fixed to the stage of a Nikon Diaphot 300 inverted light microscope. In situ microscopic examination took place daily. Photographic images of the bottom of the biofilm were captured using a 10x objective and a Nikon 35mm model N70 camera mounted on the microscope and using Kodak

400-speed black-and-white film. The pictures were then digitized using a Hewlett Packard ScanJet 4c/3c. The file format used was 768x512 8-bit gray-scale TIFF. Each pixel in the image represents a 1.04 x 1.04  $\mu\text{m}$  area.

### Digital analysis

Analysis of the digital images was conducted using a program, tentatively named Image\_Tool, developed at Montana State University over the past three years for the purpose of quantifying biofilm structure. The program was written in C++ language and designed for a Unix environment. It calculates many different structure parameters from a two-dimensional image. A few of the parameters will now be defined.

Let  $g(i,j)$  denote the  $(i,j)^{\text{th}}$  element of a normalized gray-tone spatial-dependence matrix (Haralick *et al.*, 1973). Textural Entropy, the first parameter we define, utilizes these elements; the remaining parameters use pixel values for the image after thresholding.

1. *Textural Entropy*: Textural Entropy =  $-\sum_i \sum_j g(i,j) [\ln \{g(i,j)\}]$ . It is a measure of disorganization in the image; hence, it measures heterogeneity. It has a minimum value near 0 and the theoretical maximum value depends on the gray scale used by the image capture software. High values represent more heterogeneous biofilm structures.

The remaining parameters required image manipulation called thresholding; in which the gray scale of the image is transformed into a binary scale; that is,  $p(i,j) = 0$  or 1 and there are no intermediate values. A pixel with  $p(i,j)=1$  is in a void, shaded white, and a pixel with  $p(i,j)=0$  is in a bacterial cluster, shaded black. The following parameters are calculated after the image has been thresholded.

2. *Areal Porosity*: Areal porosity =  $\sum_i \sum_j p(i,j) / [\text{total number of pixels}]$ , which is the ratio of the void area to the total area of an image. Areal porosity ranges in value from 0 to 1; the higher the value, the more pores and interstitial space within the image. Figures 1 and 2 are artificial examples of lower areal porosity and higher areal porosity images.

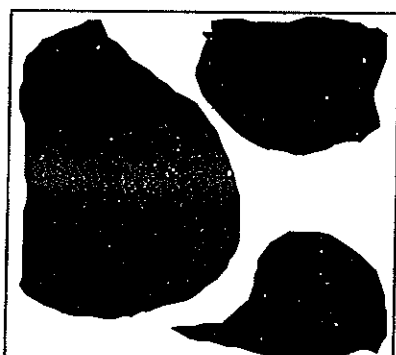


Figure 1. Example of an image that has low areal porosity.

Figure 2. Example of an image that has high areal porosity.

3. *Fractal dimension*: Fractal dimension measures the degree of raggedness of biofilm cell cluster perimeters. For a two dimensional image the fractal dimension can range from 1 to 2, where the higher the number, the more ragged the perimeter of the cluster. A straight line has fractal dimension 1, and a line so ragged that it covers a two-dimensional subplane has fractal dimension 2. The program uses the Minkowski Sausage Algorithm (Russ, 1994) to perform the calculations. Figures 3 and 4 are artificial examples of lower fractal dimension and higher fractal dimension images. The areal porosity values for the images in Figures 3 and 4 are approximately equal.

4. *Maximum diffusion distance*: The diffusion distance for an individual pixel within a cluster is the distance from that pixel to the nearest void pixel. Diffusion distances are initially calculated as "number of pixels," then converted into distances ( $\mu\text{m}$ ). They measure the distances over which the substrate has to diffuse from the void space to reach bacteria within the clusters. The maximum diffusion distance is the maximum of diffusion distances among all cluster pixels in the image. The

maximum diffusion distance for the image of Figure 2 is obviously less than that of Figure 1, whereas, the maximum diffusion distance for the images of Figures 3 and 4 is nearly equal.

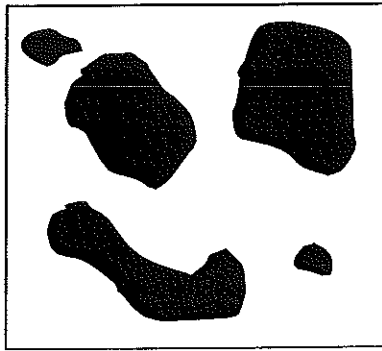


Figure 3. Example of an image that has a lower fractal dimension.

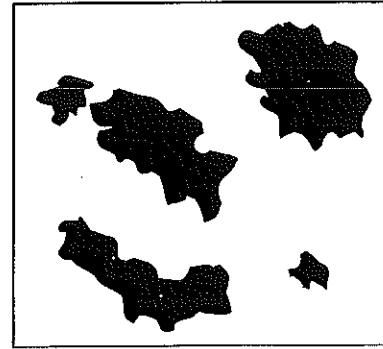


Figure 4. Example of an image that has a high fractal dimension.

### Statistical methods

All parameters were measured daily at ten randomly chosen, non-overlapping locations for a period of 18 days. For each parameter, the observed values were averaged across locations. The time series of averages were plotted separately for each parameter and a smooth line was drawn through the points to show the trend. The line was constructed by the locally weighted scatterplot smoother (LOWESS) in the Minitab (1998) computer program using the LOWESS default settings.

### RESULTS

The microscopist observed that the biofilm thickness was reaching steady state by 18 days. The time series plots of textural entropy, areal porosity, fractal dimension, and maximum diffusion distance show that the parameters were also reaching steady state (Figures 5, 6, 7, and 8) although the maximum diffusion distance had not clearly leveled out at the end of the observation period. The scatter around the smooth line provides some indication of the inherent variability of each measure. Clearly, the Maximum Diffusion Distance was the most variable of the four parameters. The fractal dimension initially decreased until day 4, then increased steadily until it flattened out at about day 15. For this three species biofilm, the cell cluster appears to have a fractal dimension of approximately 1.33 at steady state.

The entire experiment has been repeated. Preliminary analyses indicate that the general shapes and maximum values of the time series plots are repeatable (data not shown). The times at which steady states are reached varies from experiment to experiment, probably because of a variable lag phase before biofilms begin to grow to steady state.

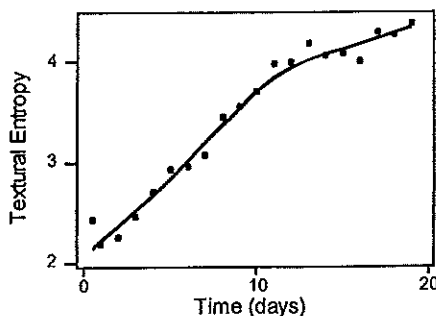


Figure 5. Textural Entropy time series.

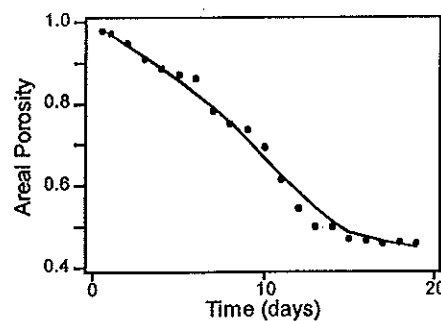


Figure 6. Areal Porosity time series.

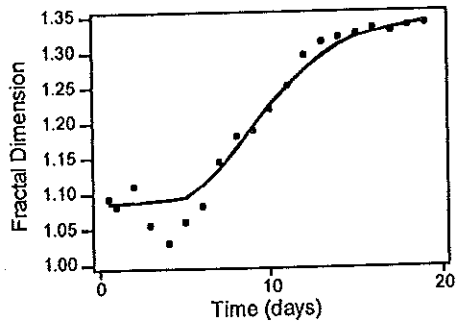


Figure 7. Fractal Dimension time series.

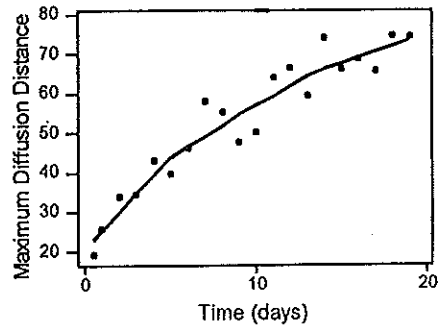


Figure 8. Max. Diffusion Distance time series.

## DISCUSSION

Structural parameters must be interpreted within the context of the size of the field viewed through the microscope. For example, if the field of view is very small, one  $\mu\text{m}$  by one  $\mu\text{m}$ , say, then at the usual power of resolution of an optical microscope, the image will show little structural heterogeneity. If we expand the field of view to  $100 \times 100 \mu\text{m}$ , then the image will show greater heterogeneity including cell clusters and interstitial voids. Expanding the field of view even more to be a few centimetres on a side, the microchannels that lie within a bacterial cell cluster may become imperceptibly small so that their contribution to heterogeneity is not detectable. The structural parameter calculations are, therefore, affected by the area of the field of view. For the data presented here, the field of view was approximately  $800 \times 530 \mu\text{m}$ , which is sufficiently large to show multiple cell clusters, but small enough to show heterogeneities at the one  $\mu\text{m}$  scale.

We have begun to collect biofilm function data for purposes of correlating the structural parameters with function. The strategy is to measure substrate concentration profiles at several points over a selected area of the biofilm using microsensors (Yang and Lewandowski, 1995; Beyenal *et al.*, 1998). From these profiles we extract substrate concentrations at certain depths within the biofilm and construct maps of substrate concentration at those selected depths. From such maps we may study the distribution of activity and we may also calculate the average activity for the whole area (field of view) and for each selected depth. Such average activities are single numbers and can be correlated with the structure quantities, as calculated from CSLM images, for the same surface area and the same depth in the biofilm.

At present, thresholding is performed subjectively by the microscopist. By watching biofilm vibrations, etc. under the microscope at the time the image is captured, the technician has a good idea where cluster boundaries are located and can set the threshold level to match those boundaries. We have conducted a special study to ascertain the statistical characteristics of the parameters and the variability of the parameters attributable to differences among technicians; the results of that study will be published elsewhere.

We constructed time series plots of parameters other than the four shown in the Results section, but they did not show clear time trends, they reached no steady-state values, or they were strongly correlated with other parameters. We will continue to investigate some of those other parameters, and we will be adding some new parameters to the Image\_Tool program.

## CONCLUSIONS

Four parameters for characterizing biofilm structure appear to reach steady-state values: textural entropy, areal porosity, fractal dimension, and maximum diffusion distance. We think that all four parameters are related to mass transfer and consequently related to function, so they have an intuitive appeal. The results suggest that it may well be possible to find quantitative parameters that are suitable for establishing structure/function correlations and for computer model evaluations.

## ACKNOWLEDGMENTS

This work was partially funded by Cooperative Agreement #EBC-8907039 between the National Science Foundation Engineering Research Centers Program and Montana State University, and by the Industrial Associates of the Center for Biofilm Engineering.

## REFERENCES

- Bishop, P. L. and Rittmann, B. E. (1995). Modelling heterogeneity in biofilms: report of the discussion session. *Wat. Sci. Tech.*, **32**(8), 263-265.
- Beyenal, H., Tanyolac, A. and Lewandowski, Z. (1998). Measurements of local effective diffusivity and cell density variations in heterogeneous biofilms. *Wat. Sci. Tech.*, **38**(8-9), 171-178.
- Costerton, J. W., Lewandowski, Z., DeBeer, D., Caldwell, D., Korber, D. and James, G. (1994). Minireview: biofilms, the customized micronich. *J. Bacteriology*, **176**(8), 2137-2142.
- Davies, D. G., Parsek, M. R., Pearson, J. P., Iglewski, B. H., Costerton, J. W. and Greenberg, E. P. (1998). The involvement of cell-to-cell signals in the development of a bacterial biofilm. *Science*, **280**, 295-298.
- DeBeer, D., Stoodley, P., Roe, F. and Lewandowski, Z. (1994). Effects of biofilm structures on oxygen distribution and mass transport. *Biotechnology and Bioengineering*, **43**, 1131-1138.
- Haralick, R. M. *et al.* (1973). Textural features for image classification. *IEEE Trans. Sys., Man., Cyber.*, **SMC-3**, 6, 610-621.
- Hermanowicz, S., Schindler, W. and Wilderer, U. (1995). Fractal structure of biofilms: new tools for investigation of morphology. *Wat. Sci. Tech.*, **32**(8), 99-105.
- Keevil, C. W. and Walker, J. T. (1992). Normarski DIC microscopy and image analysis of biofilms. *Binary*, **4**, 93-95.
- Lawrence, J. R., Korber, D. R., Hoyle, B. D., Costerton, J. W. and Caldwell, D. E. (1991). Optical sectioning of microbial biofilms. *J. Bact.*, **173**(20), 6558-6567.
- Lewandowski, Z., Stoodley, P., Altobelli, S. and Fukushima, E. (1993). Hydrodynamics and kinetics in biofilm systems - recent advances and new problems. *Wat. Sci. Tech.*, **29**(10-11), 223-229.
- Massol-Deya, A. A., Whallon, J., Hickey, R. F. and Tiedje, J. M. (1994). Channel structures in aerobic biofilms of fixed-film reactors treating contaminated groundwater. *Appl. Environ. Microbiol.*, **61**(2), 769-777.
- Minitab (1998). *Minitab Reference Manual, Release 12*. Minitab, Inc., State College, PA.
- Picioareanu, C., Van Loosdrecht, M. C. M. and Heijnen, J. J. (1998). Mathematical modeling of biofilm structure with a hybrid differential-cellular automaton approach. *Biotechnology and Bioengineering*, **58**, 101-116.
- Russ, J. (1994). *Fractal Surfaces*. Plenum, New York.
- Van Loosdrecht, M. C. M., Eikelboom, D., Gjaltema, A., Mulder, A., Tjihuis, L. and Heijnen, J. J. (1995). Biofilm structures. *Wat. Sci. Tech.*, **32**(8), 35-43.
- Wolfaardt, G. M., Lawrence, J. R., Robarts, R. D. and Caldwell, D. E. (1994). Multicellular organization in a degradative biofilm community. *Appl. Environ. Microbiol.*, **60**, 434-446.
- Yang, S. and Lewandowski, Z. (1995). Measurement of local mass transfer coefficient in biofilms. *Biotechnology and Bioengineering*, **48**, 737-744.
- Zhang, T. C. and Bishop, P. L. (1994a). Evaluation of tortuosity factors and effective diffusivities in biofilms. *Wat. Res.*, **28**, 2279-2287.
- Zhang, T. C. and Bishop, P. L. (1994b). Density, porosity, and pore structure of biofilms. *Wat. Res.*, **28**, 2267-2277.